

Pounding-involved response of isolated and non-isolated buildings under earthquake excitation

Sayed Mahmoud¹ and Robert Jankowski*²

¹*Faculty of Engineering at Mataria, Helwan University, 11718 Cairo, Egypt*

²*Faculty of Civil and Environmental Engineering, Gdansk University of Technology
ul. Narutowicza 11/12, 80-233 Gdansk, Poland*

(Received October 21, 2009, Accepted June 8, 2010)

Abstract. Previous research on pounding between seismically isolated buildings during earthquakes has been focused on impacts at the bases of structures and the effect of simultaneous interactions at the bases and at the superstructures has not been studied in details. In this paper, the seismic responses of adjacent buildings supported on different or similar base systems considering impacts between bases and superstructures are numerically investigated. The study is carried out in three parts for the two types of adjacent buildings: (i) both structures have fixed bases; (ii) one structure has fixed base and the other is seismically isolated and (iii) both structures have base isolation systems. The results of the study indicate that the pounding-involved responses of the buildings depend mainly on the type of structural base systems and on the structural parameters of both buildings. For the base-isolated building, the variation of the peak accelerations and displacements of the storeys have been found to be relatively low. On the other hand, significant differences have been observed for the fixed base building. The results of the parametric study conducted for different values of the gap size between colliding structures show the reduction in the peak base displacements as the gap distance decreases.

Keywords: structural pounding; earthquakes; seismic isolation; nonlinear modelling.

1. Introduction

The pounding-involved dynamic response of structures under earthquake excitation, which can result in severe structural damage, has recently been a subject of intensive study. A number of different methods has been proposed in order to minimize the structural response as well as the probability of collisions between adjacent buildings or bridge segments (see, for example, Xu *et al.* 1999, Zhang and Xu 1999, Jankowski *et al.* 2000, Bhaskararao and Jangid 2006, Anagnostopoulos and Karamaneas 2008). On the other hand, however, the use of seismic isolation, which is considered as one of the most promising alternatives to enhance the structural safety against earthquakes (see, Skinner *et al.* 1980, Mostaghel and Tanbakuchi 1983, Simo and Kelly 1984, Gueraud *et al.* 1985, Kelly 1986, Mostaghel and Khodaverdian 1987, Buckle and Mayes 1990, Zayas *et al.* 1990, Jangid and Datta 1995, Jangid and Londhe 1998, Komodromos 2000, Faravelli 2001), results in larger structural displacements increasing the probability of collisions.

* Corresponding author, Professor, E-mail: jankowr@pg.gda.pl

Structural pounding in isolated buildings may occur either at the foundation (base) or at the storey level if the structures with different dynamic properties are insufficiently separated. A number of analyses on pounding between seismically isolated buildings during earthquakes has been focused on impacts at the bases of structures. Tsai (1997) modelled the superstructure of a base-isolated building as a shear beam in order to study its seismic response including bumping against a rigid barrier. Malhotra (1997) performed a systematic study investigating the effect of seismic impacts between the base of an isolated building and the surrounding retaining wall. Dimova (2000) considered the energy loss in an analytical study focused on collisions in sliding systems subjected to seismic excitations. Nagarajaiah and Sun (2001) evaluated the seismic performance of the base-isolated FCC building during the 1994 Northridge earthquake with the effect of pounding. An investigation on the earthquake-induced dynamic response of the base-isolated multi-storey building considering pounding against the retaining wall was conducted by Matsagar and Jangid (2003). Komodromos *et al.* (2007) and Komodromos (2008) studied pounding between the seismically isolated building and the surrounding moat wall in order to investigate the influence of various design parameters and conditions on the peak storey accelerations and displacements.

A review of the above cited papers indicates that the conducted analyses concerned only collisions at the base level of isolated buildings. Moreover, analysed structures were usually modelled as elastic systems with linear modelling of isolation devices. Also, linear contact models were adopted to simulate pounding between adjacent structures. Therefore, the objective of the present paper is to investigate the seismic response of isolated and non-isolated buildings considering pounding at the bases as well as at the storey levels. In the analysis, the superstructures of buildings have been modelled as inelastic systems with nonlinear model of isolation devices and using nonlinear viscoelastic model of pounding force during impact.

2. System modelling

The study has been carried out in three parts for the two types of adjacent buildings: (i) both structures have fixed bases; (ii) one structure has fixed base and the other is seismically isolated and (iii) both structures have base isolation systems. In the study, the discrete elastoplastic lumped mass models of interacting three-storey buildings with isolated and non-isolated base systems have been used.

2.1 Nonlinear equations of motion

2.1.1 Two non-isolated buildings

Let m_i^l , c_i^l , u_i^l , R_i^l and m_i^r , c_i^r , u_i^r , R_i^r ($i=1,2,3$) be the masses, damping coefficients, displacements and resisting forces for the left and the right building, respectively. In the case of two structures with fixed bases (see Fig. 1), the coupling dynamic equation of motion can be written as

$$\begin{pmatrix} \mathbf{M}^l & \mathbf{0} \\ \mathbf{0} & \mathbf{M}^r \end{pmatrix} \begin{pmatrix} \ddot{\mathbf{U}}^l \\ \ddot{\mathbf{U}}^r \end{pmatrix} + \begin{pmatrix} \mathbf{C}^l & \mathbf{0} \\ \mathbf{0} & \mathbf{C}^r \end{pmatrix} \begin{pmatrix} \dot{\mathbf{U}}^l \\ \dot{\mathbf{U}}^r \end{pmatrix} + \begin{pmatrix} \mathbf{R}^l \\ \mathbf{R}^r \end{pmatrix} + \begin{pmatrix} \mathbf{F}_{ps} \\ -\mathbf{F}_{ps} \end{pmatrix} = - \begin{pmatrix} \mathbf{M}^l & \mathbf{0} \\ \mathbf{0} & \mathbf{M}^r \end{pmatrix} \begin{pmatrix} \mathbf{I} \\ \mathbf{I} \end{pmatrix} \ddot{\mathbf{u}}_g \quad (1a)$$

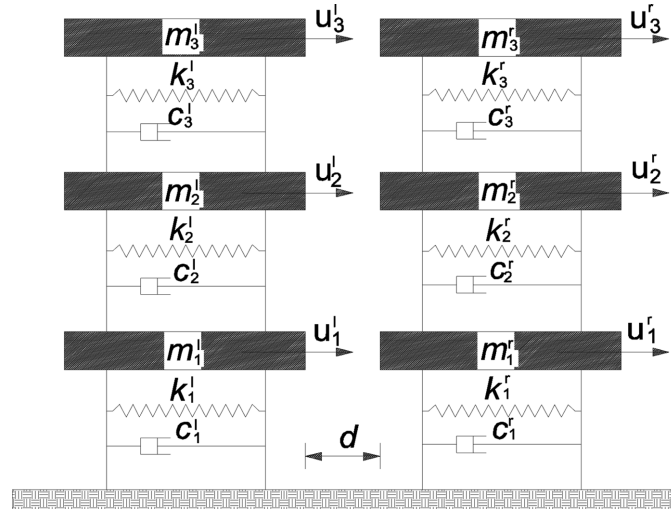


Fig. 1 Model of colliding three-storey buildings with fixed bases

$$\mathbf{M}^l = \begin{pmatrix} m_1^l & 0 & 0 \\ 0 & m_2^l & 0 \\ 0 & 0 & m_3^l \end{pmatrix}, \quad \mathbf{M}^r = \begin{pmatrix} m_1^r & 0 & 0 \\ 0 & m_2^r & 0 \\ 0 & 0 & m_3^r \end{pmatrix} \quad (1b)$$

$$\mathbf{C}^l = \begin{pmatrix} c_1^l + c_2^l & -c_2^l & 0 \\ -c_2^l & c_2^l + c_3^l & -c_3^l \\ 0 & -c_3^l & c_3^l \end{pmatrix}, \quad \mathbf{C}^r = \begin{pmatrix} c_1^r + c_2^r & -c_2^r & 0 \\ -c_2^r & c_2^r + c_3^r & -c_3^r \\ 0 & -c_3^r & c_3^r \end{pmatrix} \quad (1c)$$

$$\mathbf{R}^l = \begin{pmatrix} R_1^l - R_2^l \\ R_2^l - R_3^l \\ R_3^l \end{pmatrix}, \quad \mathbf{R}^r = \begin{pmatrix} R_1^r - R_2^r \\ R_2^r - R_3^r \\ R_3^r \end{pmatrix}, \quad \mathbf{F}_{ps} = \begin{pmatrix} F_{11} \\ F_{22} \\ F_{33} \end{pmatrix} \quad (1d)$$

$$\mathbf{U}^l = \begin{pmatrix} u_1^l \\ u_2^l \\ u_3^l \end{pmatrix}, \quad \dot{\mathbf{U}}^l = \begin{pmatrix} \dot{u}_1^l \\ \dot{u}_2^l \\ \dot{u}_3^l \end{pmatrix}, \quad \ddot{\mathbf{U}}^l = \begin{pmatrix} \ddot{u}_1^l \\ \ddot{u}_2^l \\ \ddot{u}_3^l \end{pmatrix} \quad (1e)$$

$$\mathbf{U}^r = \begin{pmatrix} u_1^r \\ u_2^r \\ u_3^r \end{pmatrix}, \quad \dot{\mathbf{U}}^r = \begin{pmatrix} \dot{u}_1^r \\ \dot{u}_2^r \\ \dot{u}_3^r \end{pmatrix}, \quad \ddot{\mathbf{U}}^r = \begin{pmatrix} \ddot{u}_1^r \\ \ddot{u}_2^r \\ \ddot{u}_3^r \end{pmatrix} \quad (1f)$$

where \mathbf{M}^l , \mathbf{C}^l and \mathbf{M}^r , \mathbf{C}^r , are the mass and damping matrices of the left and the right building, respectively; \mathbf{R}^l and \mathbf{R}^r are vectors consisting of the system resisting forces; \mathbf{U}^l , $\dot{\mathbf{U}}^l$, $\ddot{\mathbf{U}}^l$ and \mathbf{U}^r , $\dot{\mathbf{U}}^r$, $\ddot{\mathbf{U}}^r$ denote the displacement, velocity and acceleration vectors of the left and the right structure, respectively; \mathbf{F}_{ps} is a vector containing the forces due to impact; \mathbf{I} is a vector with all its elements equal to unity and \ddot{u}_g is the earthquake acceleration. During the elastic stage, resisting forces, R_i^l , R_i^r , take the form: $R_i^l = k_i^l(u_i^l - u_{i-1}^l)$, $R_i^r = k_i^r(u_i^r - u_{i-1}^r)$, while during the plastic stage: $R_i^l = \pm f_{yi}^l$, $R_i^r = \pm f_{yi}^r$,

where k_i^l , k_i^r and f_{yi}^l , f_{yi}^r are the storey stiffness coefficients and yield forces for the left and the right building, respectively.

2.1.2 One isolated and one non-isolated building

In the case of one base-isolated and one fixed building (see Fig. 2), the inelastic equation of motion (1) is additionally coupled with the following equation related to the movement of the isolated base of the left structure

$$m_b^l \ddot{u}_b^l + F_b^l + F_{pb}^l = -m_b^l \ddot{u}_g \quad (2)$$

where, m_b^l , \ddot{u}_b^l is the mass and acceleration of the base of the left building, respectively, F_b^l is the restoring force of the isolation system and F_{pb}^l is the pounding force at the base level of the left building.

2.1.3 Two isolated buildings

In the case of two base-isolated buildings (see Fig. 3), the inelastic equation of motion (1) is additionally coupled with the following equation related to the movement of the isolated bases of the left and the right structure

$$\begin{pmatrix} m_b^l & 0 \\ 0 & m_b^r \end{pmatrix} \begin{pmatrix} \ddot{u}_b^l \\ \ddot{u}_b^r \end{pmatrix} + \begin{pmatrix} F_b^l \\ F_b^r \end{pmatrix} + \begin{pmatrix} F_{pb}^l \\ -F_{pb}^r \end{pmatrix} = - \begin{pmatrix} m_b^l & 0 \\ 0 & m_b^r \end{pmatrix} \begin{pmatrix} \ddot{u}_g \\ \ddot{u}_g \end{pmatrix} \quad (3)$$

where m_b^r , \ddot{u}_b^r is the mass and acceleration of the base of the right building, respectively, F_b^r is the restoring force of the isolation system and F_{pb}^r is the pounding force at the base level of the right building.

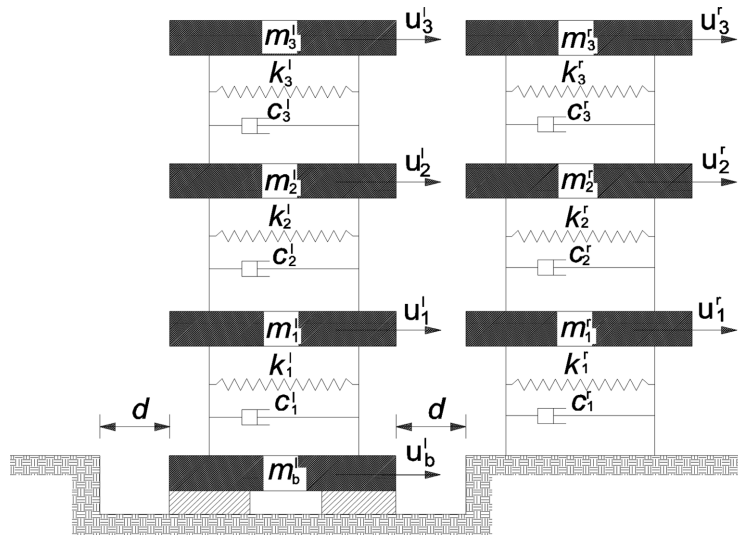


Fig. 2 Model of colliding three-storey buildings with isolated and non-isolated bases

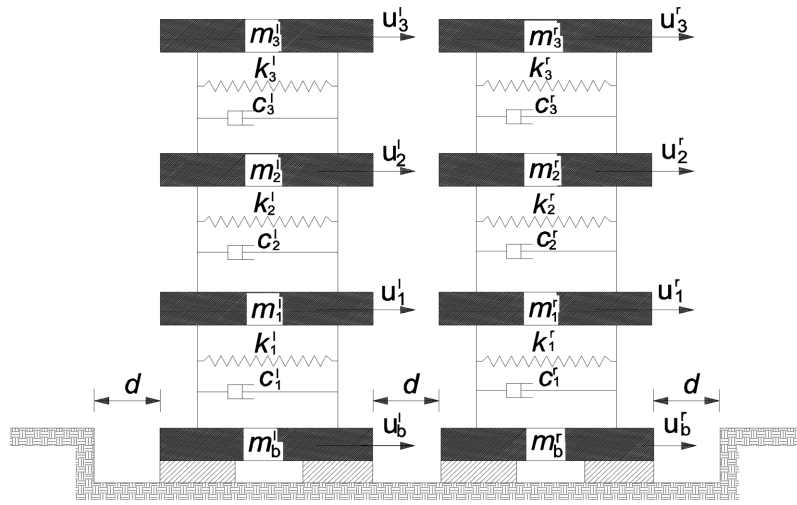


Fig. 3 Model of colliding three-storey base-isolated buildings

2.2 Nonlinear model of isolation system

Seismic isolation of structures provides the mitigation of seismic damage of structures being a reliable and cost-effective method. Among the developed various types of isolation systems, the use of High Damping Rubber Bearings (HDRBs) is one of the most attractive solutions. These bearings have also been used in this study as the isolation devices. In order to simulate the behaviour of HDRBs, a nonlinear strain rate dependent model (see, Jankowski 2003) has been applied. The model describes the behaviour of the bearing by a nonlinear elastic spring-dashpot element. The restoring force of HDRB is expressed as

$$F_b = k_b u_b + c_b \dot{u}_b \quad (4)$$

where k_b , c_b are the stiffness and damping coefficients, obtained at a given time based on the actual values of displacement, u_b , and velocity, \dot{u}_b , using formulas (Jankowski 2003)

$$k_b = a_1 + a_2(u_b)^2 + a_3(u_b)^4 + \frac{a_4}{\cosh^2(a_5 \dot{u}_b)} + \frac{a_6}{\cosh(a_7 \dot{u}_b) \cosh(a_8 \dot{u}_b)} \quad (5a)$$

$$c_b = \frac{a_9 + a_{10}(u_b)^2}{\sqrt{a_{11}^2 + (\dot{u}_b)^2}} \quad (5b)$$

where a_1 - a_{11} are parameters of the model which are obtained by fitting the experimental data using the method of the least squares.

2.3 Nonlinear model for pounding simulation

Pounding between adjacent structures is a highly complex phenomenon. Therefore, in order to accurately simulate impact, an appropriate impact force model must be adopted. Two recently

proposed pounding force models, i.e. the nonlinear viscoelastic model (Jankowski 2005) and the Hertz damp model (Muthukumar and DesRoches 2006), use the general trend of the nonlinear Hertz law of contact, in which a hysteretic damping function is additionally incorporated so as to simulate the dissipation of energy during impact. The results of the comparative study conducted for different ground motion records with different peak ground accelerations show that the nonlinear viscoelastic model is more accurate in capturing the pounding force (see Mahmoud *et al.* 2008 for details). Therefore, this model has been employed in the analysis of earthquake-induced pounding between adjacent buildings presented in this paper. According to the nonlinear viscoelastic model, the value of pounding force between the i th ($i=1,2,3$) storeys of two adjacent buildings is calculated as (Jankowski 2005)

$$\begin{aligned}
 F_{ii} &= 0 \quad \text{for } \delta_{ii} \leq 0 \quad (\text{no contact}) \\
 F_{ii} &= \bar{\beta} \delta_{ii}^{\frac{3}{2}} + \bar{c}_{ii} \dot{\delta}_{ii} \quad \text{for } \delta_{ii} > 0 \text{ and } \dot{\delta}_{ii}(t) > 0 \quad (\text{contact-approach period}) \\
 F_{ii} &= \bar{\beta} \delta_{ii}^{\frac{3}{2}} \quad \text{for } \delta_{ii} > 0 \text{ and } \dot{\delta}_{ii}(t) \leq 0 \quad (\text{contact-restitution period})
 \end{aligned} \tag{6}$$

where $\delta_{ii} = (u_i^l - u_i^r - d)$ is the relative displacement (d denotes the initial separation gap), $\bar{\beta}$ is the impact stiffness parameter and

$$\bar{c}_{ii} = 2\bar{\xi} \sqrt{\bar{\beta} \sqrt{\delta_{ii}} \frac{m_i^l m_i^r}{m_i^l + m_i^r}} \tag{7}$$

is the impact element's damping. Here, $\bar{\xi}$ is an impact damping ratio related to a coefficient of restitution, e , which can be defined as (Jankowski 2006)

$$\bar{\xi} = \frac{9\sqrt{5}}{2} \frac{1 - e^2}{e(9\pi - 16) + 16} \tag{8}$$

3. Response to earthquake excitation

In the study, the seismic response of adjacent three-storey buildings with isolated and non-isolated bases considering pounding effect has been investigated. The feasibility of the study has been demonstrated by a series of numerical simulations. A parametric study has been carried out for a number of cases, including base type, different parameters of the storeys mass, stiffness, damping coefficients and yielding forces. A number of different cases for pounding between isolated and non-isolated building systems has been analyzed for different separation distances between the adjacent buildings. The NS components of the El Centro earthquake (18.05.1940, PGA = 0.34 g , g is the acceleration of gravity), the Cape Mendocino earthquake (25.04.1992, PGA = 0.59 g) and the Kobe earthquake (17.01.1995, PGA = 0.82 g) have been considered in this study. In the case of the El Centro earthquake, together with the original record, two scaled records (PGA = 0.60 g and PGA = 0.90 g) have also been applied.

3.1 Nonlinear system parameters

The dynamic parameters of superstructures of buildings considered in the study are shown in Table 1 (Jankowski 2008). These parameters make the superstructure of one of the buildings to be more flexible and lighter when compared to the other one, which is stiffer and heavier. The fundamental natural periods of the non-isolated structures have been calculated as equal to 1.2 s and 0.30 s for the flexible and stiff building, respectively.

The base-isolated building with flexible superstructure has been equipped with 4 circular HDRBs with the following parameters of the bearing's model (see example 3 in Jankowski 2003): $a_1 = 4.1051 \cdot 10^5$ N/m, $a_2 = -1.7238 \cdot 10^3$ N/m³, $a_3 = -98.611$ N/m⁵, $a_4 = 1.2261 \cdot 10^5$ N/m, $a_5 = 5.0777$ s/m, $a_6 = 3.5740 \cdot 10^5$ N/m, $a_7 = 6.9069$ s/m, $a_8 = 48.371$ 1/m, $a_9 = 1.0169 \cdot 10^4$ N, $a_{10} = 8.0471 \cdot 10^4$ N/m², $a_{11} = 0.15621$ m/s. On the other hand, the base-isolated building with stiff superstructure has been equipped with 4 square HDRBs with the following parameters of the bearing's model (see example 1 in Jankowski 2003): $a_1 = 7.5509 \cdot 10^6$ N/m, $a_2 = 3.8939 \cdot 10^6$ N/m³, $a_3 = 1.3423 \cdot 10^8$ N/m⁵, $a_4 = 3.1749 \cdot 10^6$ N/m, $a_5 = 1.4906$ s/m, $a_6 = 2.8303 \cdot 10^7$ N/m, $a_7 = 7.1213$ s/m, $a_8 = 45.693$ 1/m, $a_9 = 4.9075 \cdot 10^5$ N, $a_{10} = 2.2888 \cdot 10^6$ N/m², $a_{11} = 0.58681$ m/s. The following parameters of the nonlinear viscoelastic model of pounding force have also been applied in the analysis: $\bar{\beta} = 2.75 \cdot 10^9$ N/m^{3/2}, $\xi = 0.35$ ($e = 0.65$) (see Jankowski 2008).

3.2 Solution procedure

The Newmark method with a constant step size of 0.001s has been used to solve the equations of motion. In order to attain high degree of numerical stability, the constant average acceleration approach with $\gamma = 0.5$ and $\beta = 0.25$ has been applied. The numerical simulations have been performed using MATLAB 7.0 software on a Dell PC with 2 MB memory and 800 MHz.

3.3 Case studies

3.3.1 Pounding between two non-isolated buildings

First, the pounding-involved seismic response of two buildings with non-isolated bases (see Fig. 1) has been investigated. In the analysis, the left building has been considered to be a flexible one, whereas the right structure to be a stiff one. The results of the analysis in the form of the peak displacements, accelerations and pounding forces with respect to the gap size between structures are presented in Figs. 4 and 5. It can be seen from the figures that the peak displacements and accelerations for the right building (stiffer and heavier one) show almost constant values for all gap

Table 1 Properties of superstructures of buildings used in the study

Storey parameter	Building with flexible superstructure	Building with stiff superstructure
Mass	$25 \cdot 10^3$ kg	10^6 kg
Damping	5%	5%
Stiffness	$3.46 \cdot 10^6$ N/m	$2.215 \cdot 10^9$ N/m
Yielding force	$1.369 \cdot 10^5$ N	$1.589 \cdot 10^7$ N

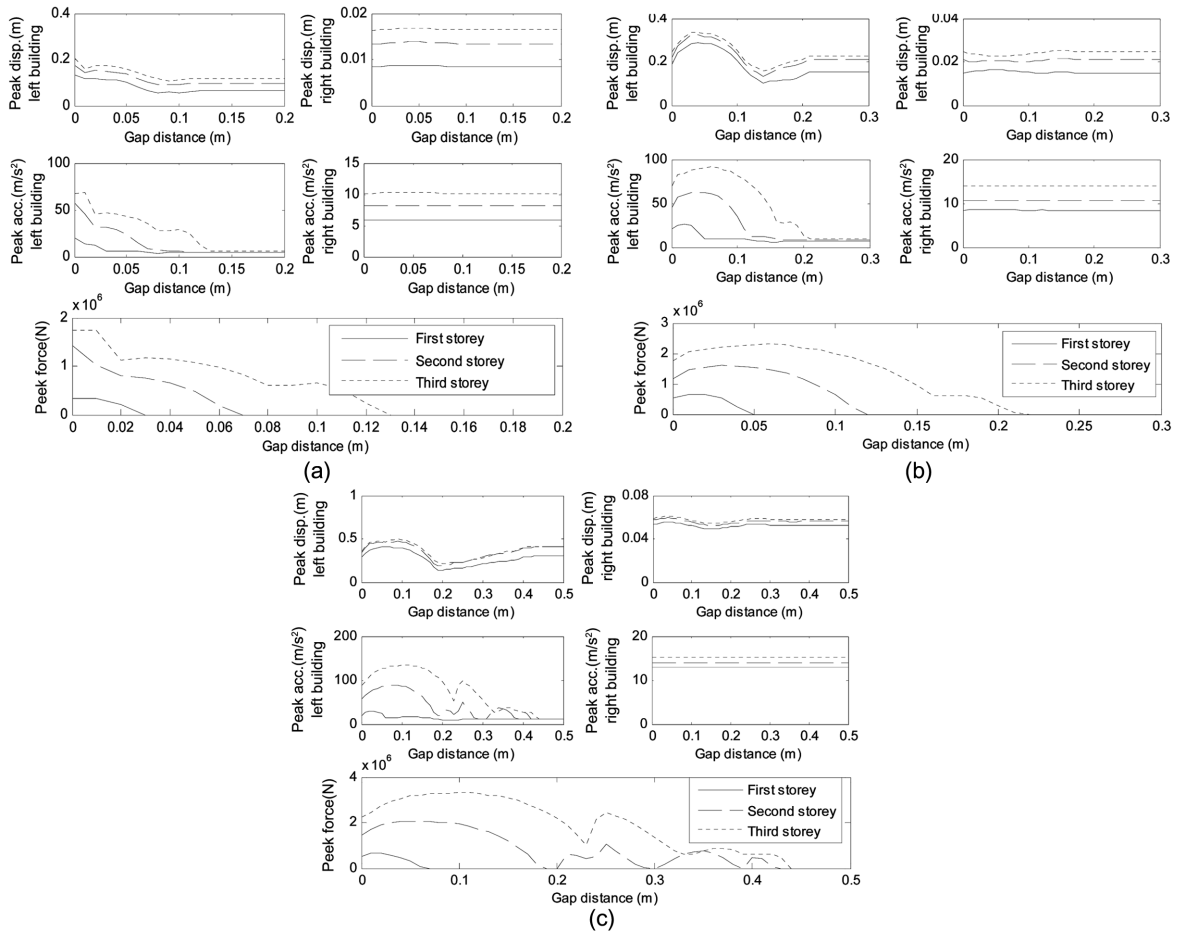


Fig. 4 Peak displacements, accelerations and pounding forces with respect to the gap distance between adjacent non-isolated buildings under: (a) the original El Centro earthquake, (b) the El Centro earthquake scaled to $\text{PGA} = 0.6 g$, (c) the El Centro earthquake scaled to $\text{PGA} = 0.9 g$

distances and earthquake excitations. On the other hand, the results obtained for the left building (more flexible and lighter one) indicate that collisions lead to significant changes in its response. For the original El Centro earthquake (see Fig. 4(a)) and for the Cape Mendocino earthquake (see Fig. 5(a)), the peak displacements and accelerations of the storeys of the left building decrease with the increase in the separation distance. Similar relation concerns also the peak pounding force. For the El Centro earthquake scaled to $\text{PGA} = 0.6 g$ (see Fig. 4(b)) and for the Kobe earthquake (see Fig. 5(b)), it is observed that there is an initial increase in the peak storeys displacements, accelerations as well as pounding forces followed by a decrease trend. On the other hand, a non uniform increase and decrease trend in the peak values of the displacements, accelerations and pounding forces can be observed for the relatively high PGA of $0.90 g$ of the El Centro record (see Fig. 4(c)).

3.3.2 Pounding between one isolated and one non-isolated building

In this section, structural pounding between one isolated and one non-isolated building is investigated (see Fig. 2). The following three cases have been considered in the analysis: (i) both

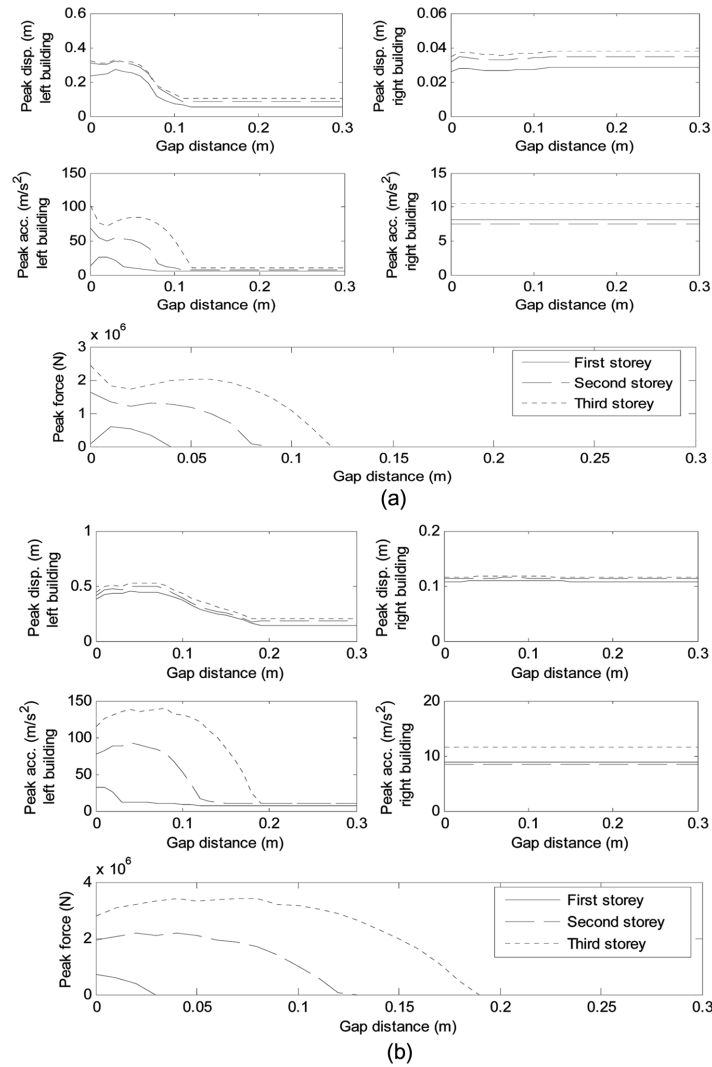


Fig. 5 Peak displacements, accelerations and pounding forces with respect to the gap distance between adjacent non-isolated buildings under: (a) the Cape Mendocino earthquake, (b) the Kobe earthquake

buildings have stiff superstructures, (ii) both buildings have flexible superstructures, (iii) the isolated building has flexible superstructure while the non-isolated building is stiff, (iv) the isolated building has stiff superstructure while the non-isolated building is flexible.

3.3.2.1 Case (i)

The results of the analysis for the case of two buildings with stiff superstructures are shown in Figs. 6 and 7. It can be seen from the figures that the storeys peak responses of the base-isolated building (the left one) are significantly different comparing to the responses of the non-isolated structure (the right one). The peak displacements and accelerations of the storeys of the isolated building are considerably higher than the ones obtained for the non-isolated structure. The results indicate that the response values of the isolated building increase up to a certain value of the gap

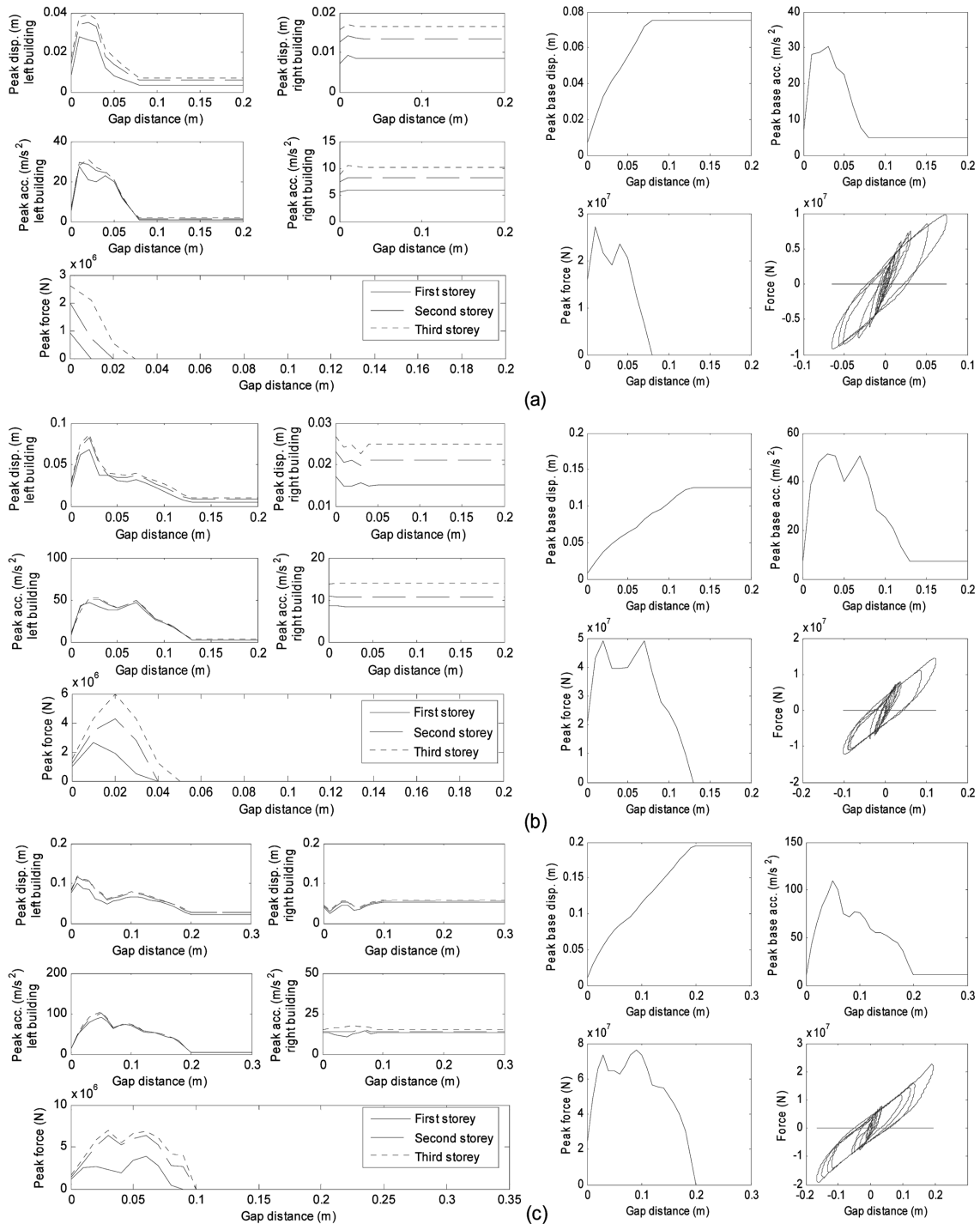


Fig. 6 Peak displacements, accelerations and pounding forces with respect to the gap distance between isolated and non-isolated buildings with stiff superstructures under: (a) the original El Centro earthquake, (b) the El Centro earthquake scaled to $PGA = 0.6 g$, (c) the El Centro earthquake scaled to $PGA = 0.9 g$

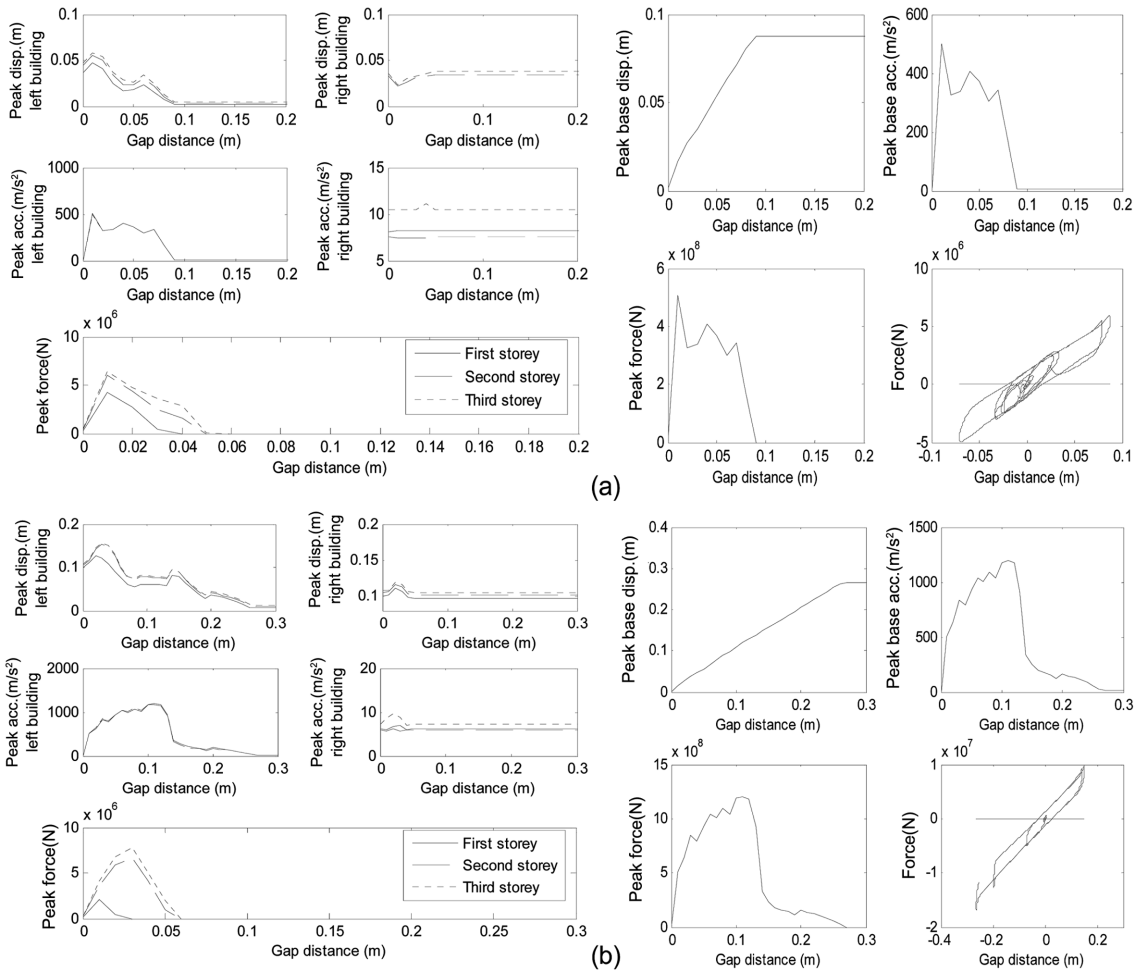


Fig. 7 Peak displacements, accelerations and pounding forces with respect to the gap distance between isolated and non-isolated buildings with stiff superstructures under: (a) the Cape Mendocino earthquake, (b) the Kobe earthquake

distance and a significant reduction in peak displacements and accelerations with further increase in the gap distance can be observed for all considered earthquake excitations. On the other hand, the storeys of the non-isolated building show almost constant values of peak displacements and accelerations for all considered gap distances and ground motions. Moreover, the lower and higher storeys of the base-isolated left building induce approximately similar peak displacements and accelerations under all PGA levels of the same ground motion and separation distances considered in the analysis (see Fig. 6). The peak pounding forces induced at higher storey levels are of high values compared with those induced at lower storey levels. It has also been noticed that the peak pounding forces at the bearing level increase up to a certain value of the gap distance and with further increase in the gap distance a decrease trend can be observed for all considered earthquake excitations (see Figs. 6 and 7). Similar trend can be seen for the peak accelerations obtained at different separation distances. Moreover, the results of the study show that the base peak displacements increase with the increase in the gap distance.

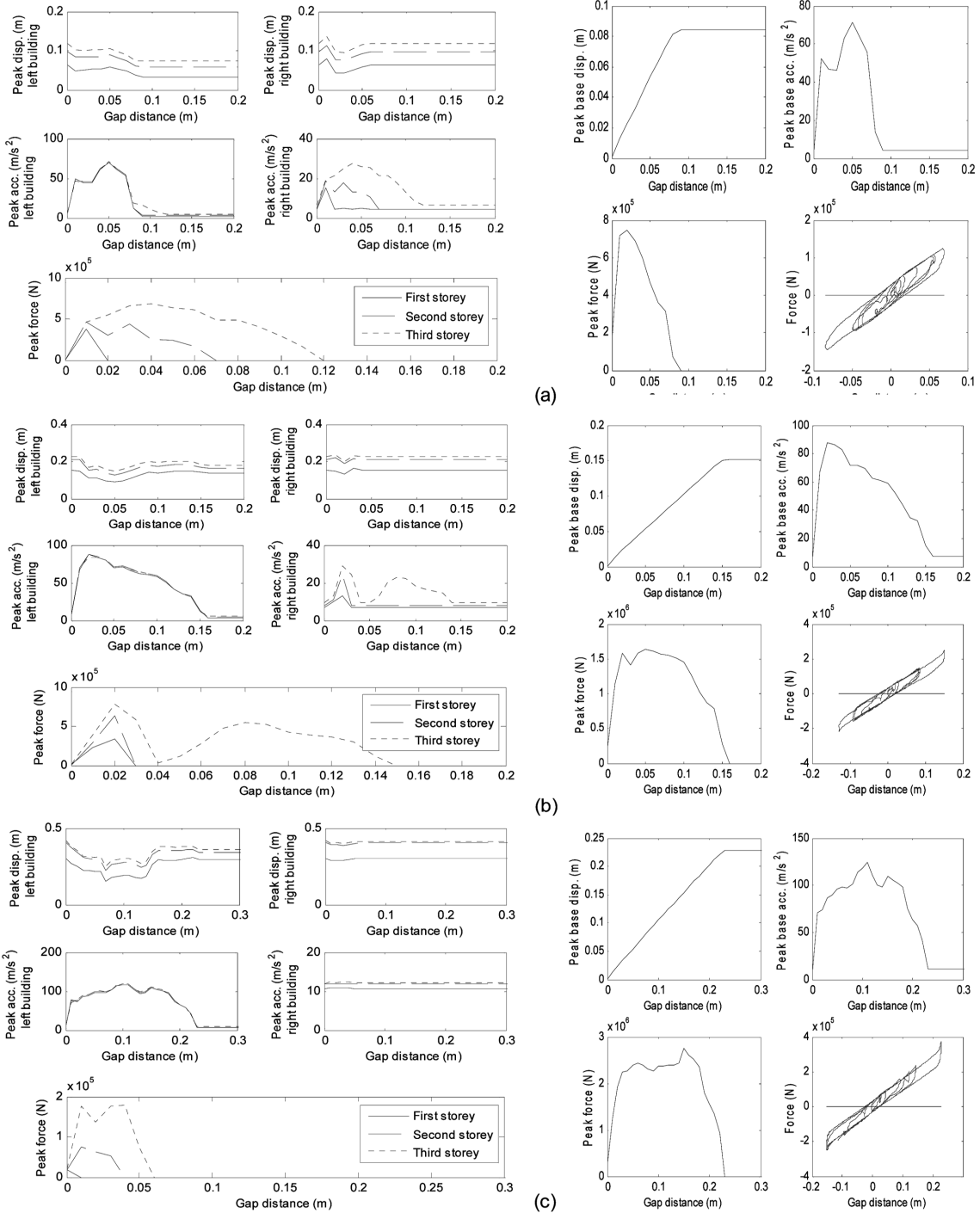


Fig. 8 Peak displacements, accelerations and pounding forces with respect to the gap distance between isolated and non-isolated buildings with flexible superstructures under: (a) the original El Centro earthquake, (b) the El Centro earthquake scaled to PGA = 0.6 g, (c) the El Centro earthquake scaled to PGA = 0.9 g

3.3.2.2 Case (ii)

The results of the analysis for the case of two buildings with flexible superstructures are shown in Figs. 8 and 9. It can be seen from the figures that the non-isolated building (the right one) provide approximately constant peak displacements for all ground motions and gap distances considered in the study. The peak pounding forces at the storey levels of this structure increase up to a certain value of the gap distance and with further increase in the gap distance a decrease trend can be

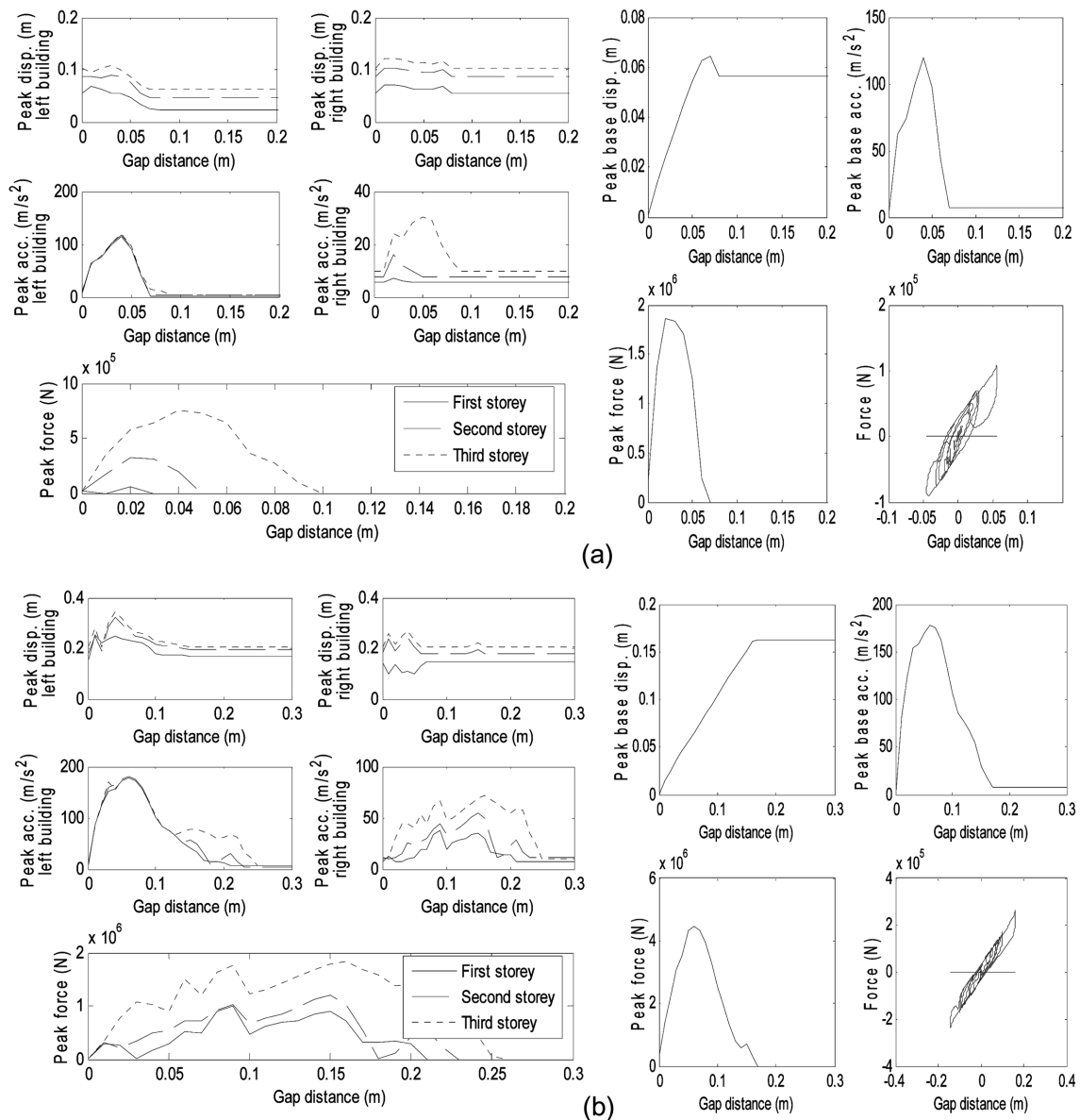


Fig. 9 Peak displacements, accelerations and pounding forces with respect to the gap distance between isolated and non-isolated buildings with flexible superstructures under: (a) the Cape Mendocino earthquake, (b) the Kobe earthquake

observed. Moreover, the peak pounding forces induced at higher storey levels are of higher values comparing with those induced at lower storey levels. The storeys peak accelerations of the non-isolated building are somehow proportional to the pounding forces exerted on the superstructures. For the base-isolated building (the left one), the decrease in the peak displacements with the gap distance increase is observed for the El Centro record with $PGA = 0.34 g$ and for the Cape Mendocino earthquake. On the other hand, for the two other PGA levels (i.e. $0.60 g$ and $0.90 g$) of the El Centro earthquake a decrease in the peak displacements followed by an increase trend has been recorded, while for the Kobe ground motion an opposite trend can be seen in Fig. 9(b). All the storeys of the base-isolated building have approximately the same values of the peak accelerations obtained under all types of excitations and separation distances considered in the analysis. These values of storeys peak accelerations increase up to a certain value of the gap distance and with further increase in the gap distance a decrease trend can be observed (see Figs. 8 and 9). The peak responses of the base of isolated building show similar behaviour as those described for the case (i).

3.3.2.3 Case (iii)

In this case we have considered pounding between the isolated building with flexible superstructure (the left one) and the non-isolated stiff building (the right one). The peak displacements, accelerations and pounding forces with respect to the gap distance between the structures under the El Centro earthquake record scaled to different PGA levels are shown in Fig. 10, while under the Cape Mendocino and the Kobe earthquakes are presented in Fig. 11. It can be seen from the figures that the non-isolated stiff building shows almost constant peak displacements and accelerations for all the excitations and gap distances considered in the study. On the other hand, the peak displacements and accelerations for the storeys of the isolated building with flexible superstructure show larger differences. In the case of the original ground motion record of the El Centro earthquake (Fig. 10(a)) as well as for the Kobe earthquake (Fig. 11(b)), an increase up to a certain value of the gap distance is observed and with further increase in the gap distance a decrease trend has been recorded. For the two scaled records of the El Centro ground motion and for the Cape Mendocino earthquake, the storeys peak displacements and accelerations show non-uniform increase and decrease trend. All the storeys of the base-isolated left building provide almost identical peak displacements and accelerations for all the considered gap distances. The impact forces have a decrease tendency with the increase in the gap distance showing significant differences between higher and lower storey levels. Moreover, it has been noticed that the peak pounding forces at the base level of isolated building increase up to a certain value of the gap distance and with further increase in the gap distance a decrease trend can be observed for all considered ground motions. Similar trend can be seen for the peak accelerations obtained at different separation distances. On the other hand, the base peak displacements increase with the increase in the gap distance between buildings.

3.3.2.4 Case (iv)

In the last case of this section, pounding between the isolated building with stiff superstructure (the left one) and the non-isolated flexible building (the right one) has been considered. The peak displacements, accelerations and pounding forces with respect to the gap distance between the structures under the El Centro earthquake record scaled to different PGA levels as well as under the Cape Mendocino and the Kobe earthquakes are shown in Figs. 12 and 13. The results indicate that

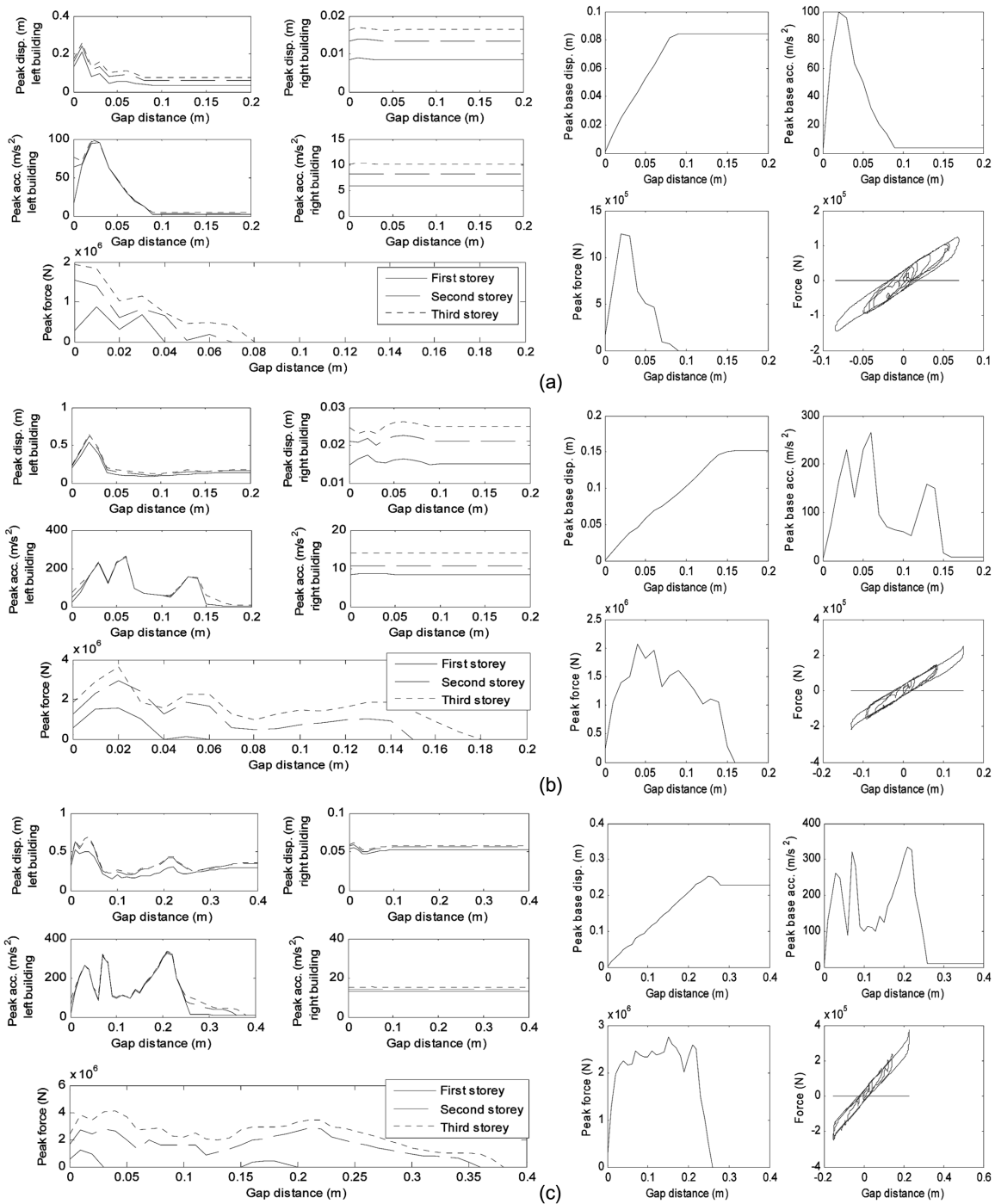


Fig. 10 Peak displacements, accelerations and pounding forces with respect to the gap distance between isolated building with flexible superstructure and non-isolated stiff building under: (a) the original El Centro earthquake, (b) the El Centro earthquake scaled to PGA = 0.6g, (c) the El Centro earthquake scaled to PGA = 0.9g

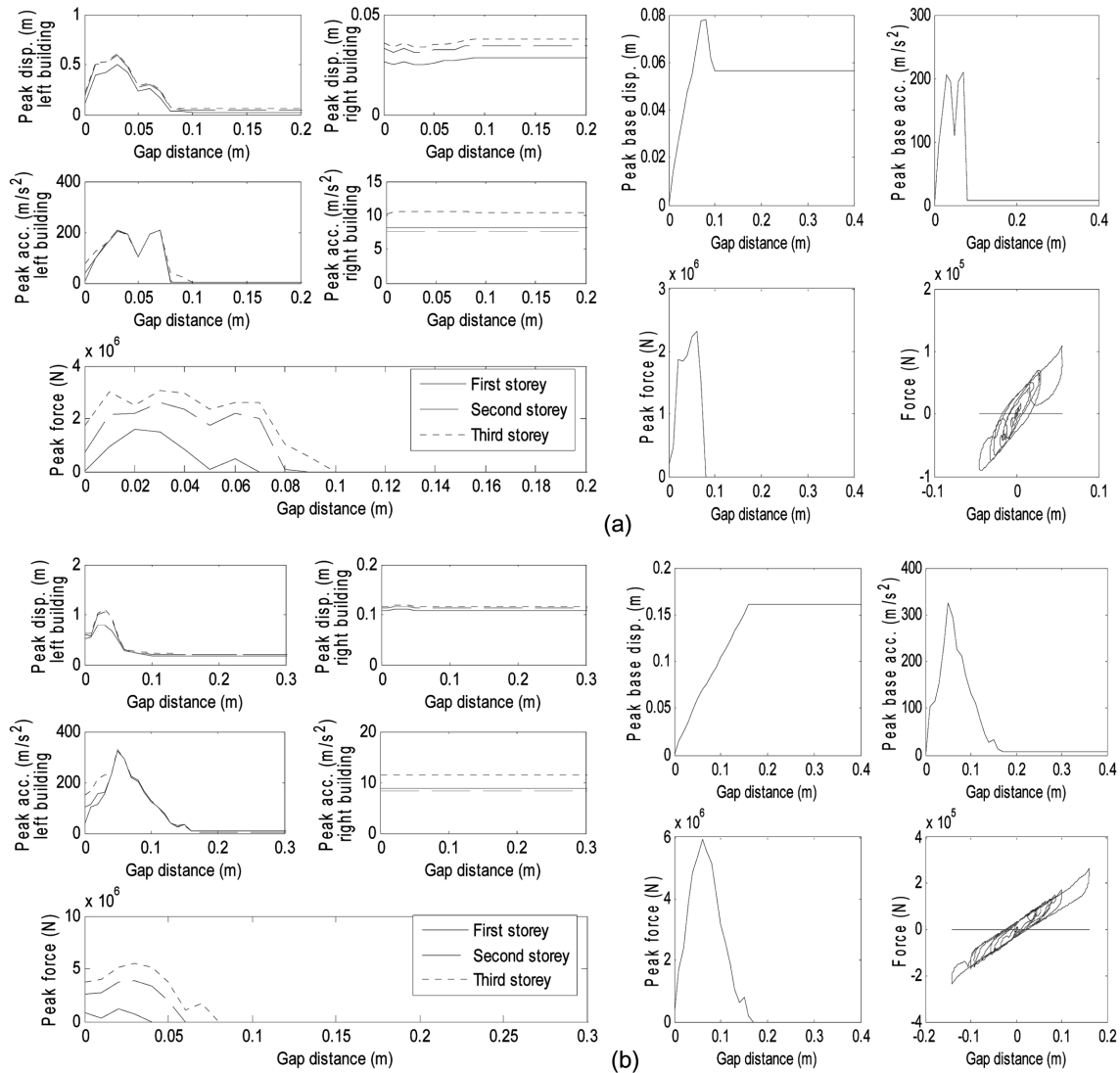


Fig. 11 Peak displacements, accelerations and pounding forces with respect to the gap distance between isolated building with flexible superstructure and non-isolated stiff building under: (a) the Cape Mendocino earthquake, (b) the Kobe earthquake

the peak displacements and accelerations for the storeys of the isolated building with stiff superstructure increase up to a certain value of the gap distance and with further increase in the gap distance a decrease trend can be observed for all ground motions. In addition, all the storeys provide almost identical peak displacement and acceleration responses for all the considered gap distances. For the non-isolated right building, the peak displacements and accelerations normally decrease with the increase in the separation distance providing significant differences between the responses of the lower and higher storeys. The peak pounding forces follow a similar trend as the peak displacements and accelerations obtained for the non-isolated flexible building. It has also been noticed that the peak pounding forces at the base level of isolated building increase up to a certain

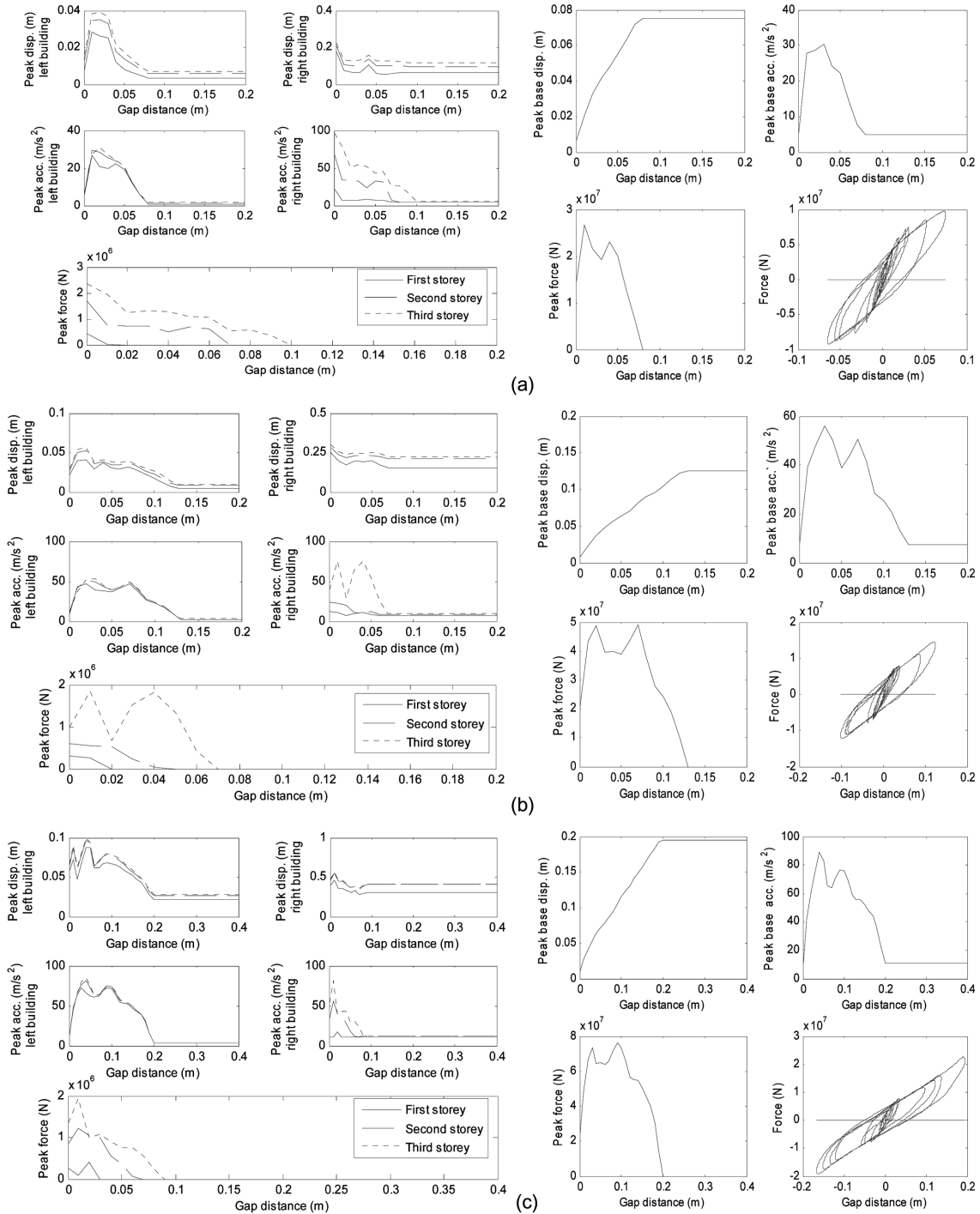


Fig. 12 Peak displacements, accelerations and pounding forces with respect to the gap distance between isolated building with stiff superstructure and non-isolated flexible building under: (a) the original El Centro earthquake, (b) the El Centro earthquake scaled to PGA = 0.6 g, (c) the El Centro earthquake scaled to PGA = 0.9g

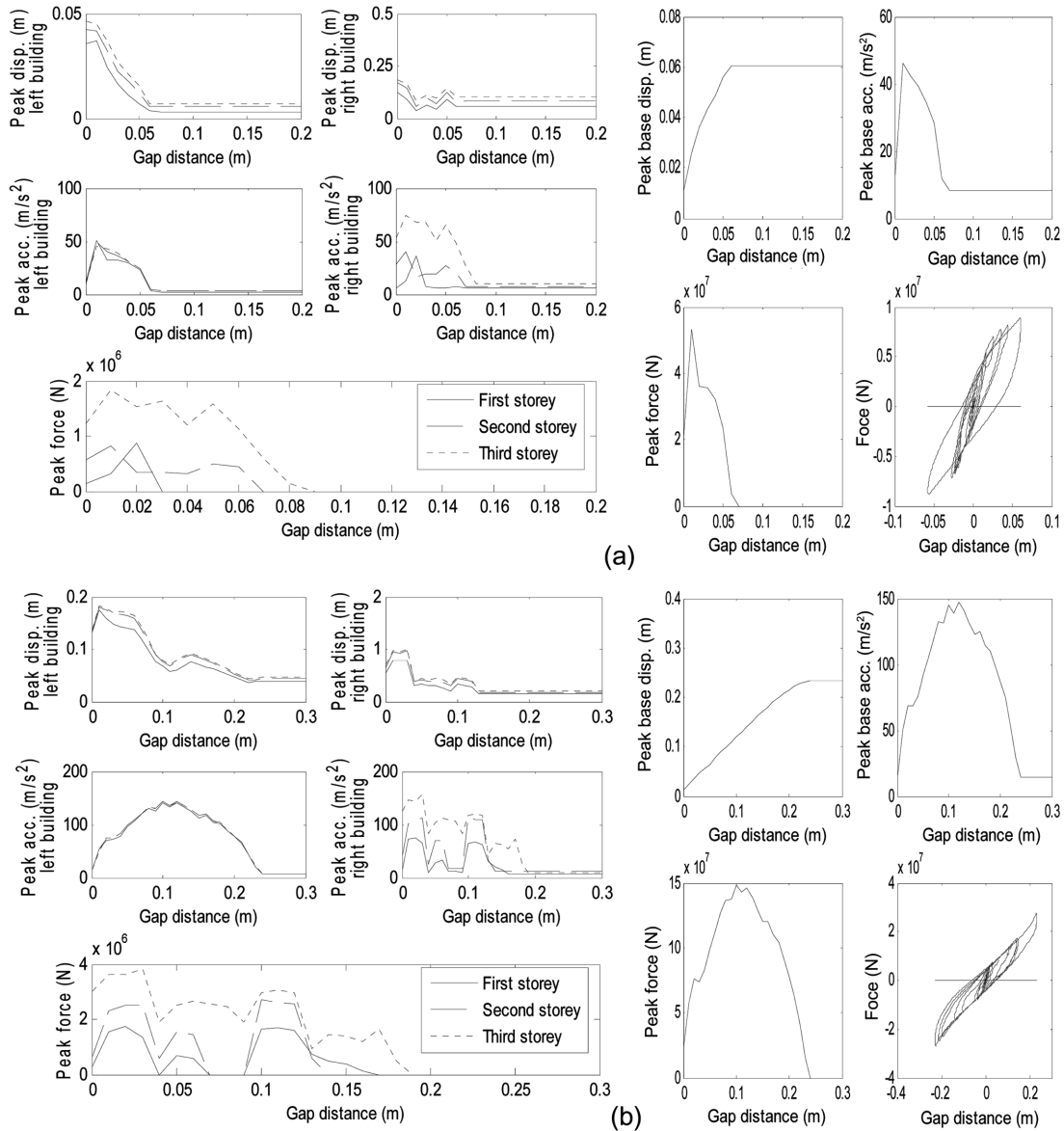


Fig. 13 Peak displacements, accelerations and pounding forces with respect to the gap distance between isolated building with stiff superstructure and non-isolated flexible building under: (a) the Cape Mendocino earthquake, (b) the Kobe earthquake

value of the gap distance and with further increase in the gap distance a decrease trend can be observed for all considered earthquake excitations. Similar trends can also be seen for the peak accelerations obtained at different separation distances.

3.3.3 Pounding between two isolated buildings

Finally, the pounding-involved seismic response of two buildings with isolated bases (see Fig. 3) has been considered. Similarly as in section 3.3.1, the left building has been assumed to have

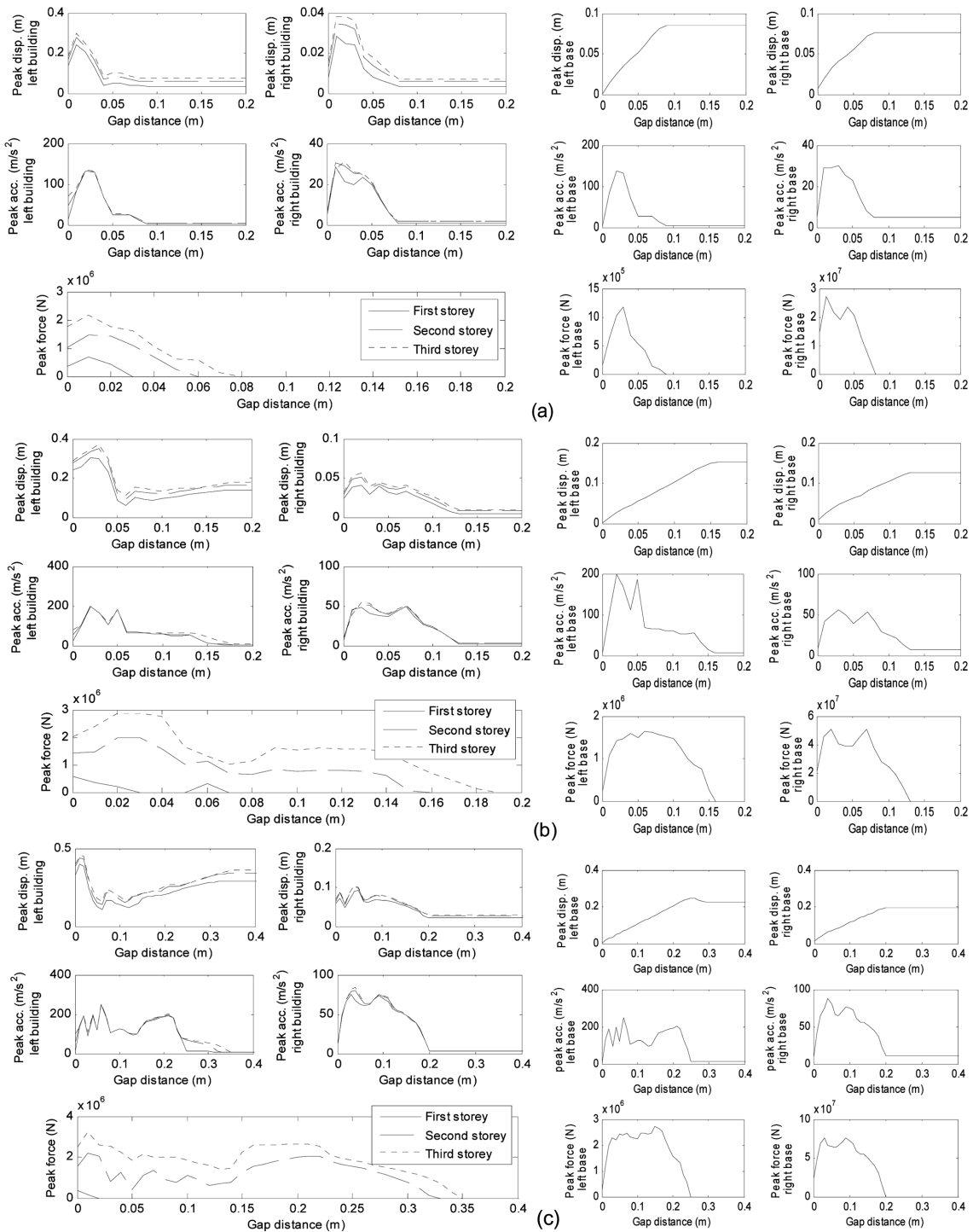


Fig. 14 Peak displacements, accelerations and pounding forces with respect to the gap distance between adjacent isolated buildings under: (a) the original El Centro earthquake, (b) the El Centro earthquake scaled to $PGA = 0.6 g$, (c) the El Centro earthquake scaled to $PGA = 0.9 g$

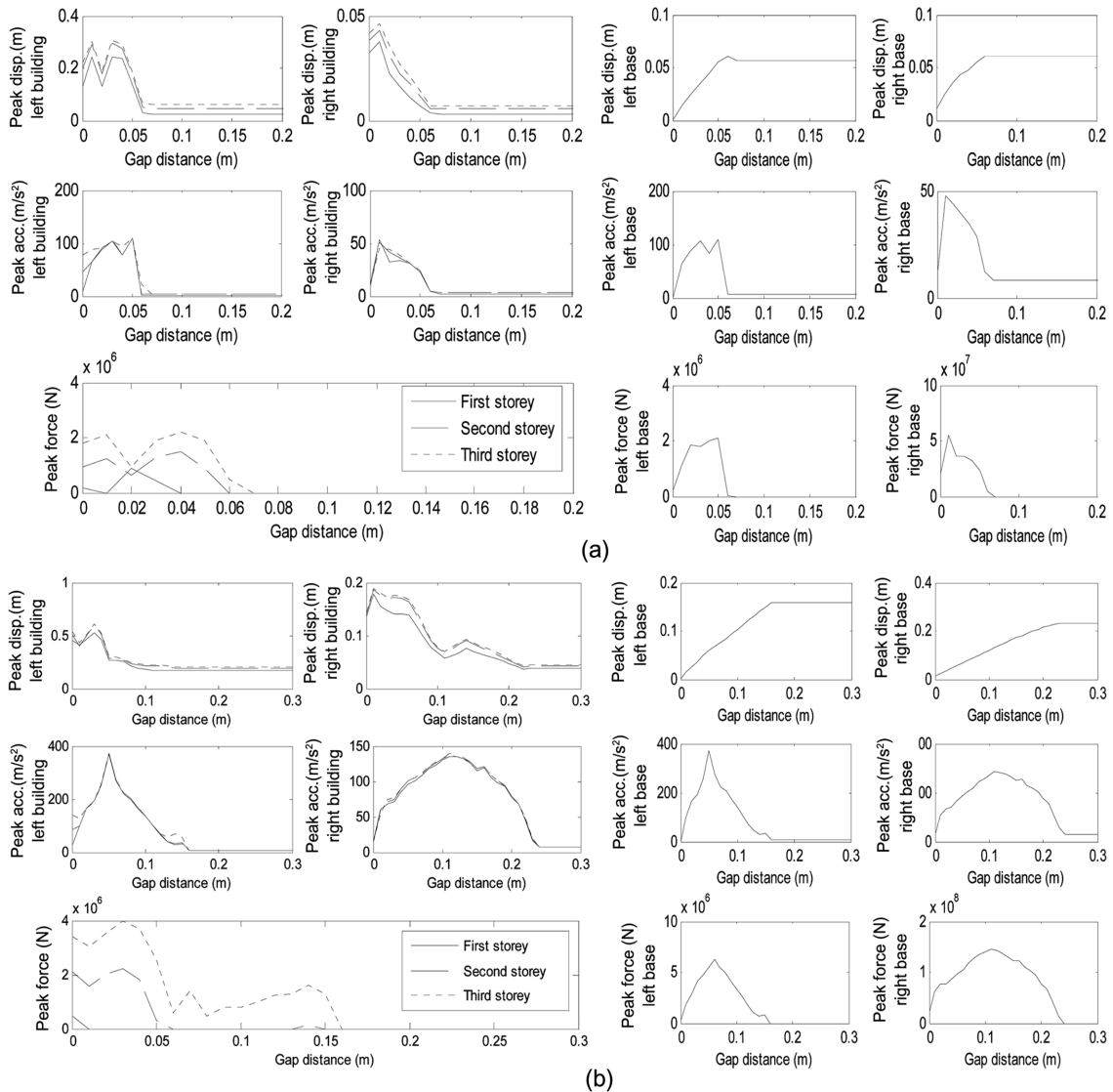


Fig. 15 Peak displacements, accelerations and pounding forces with respect to the gap distance between adjacent isolated buildings under: (a) the Cape Mendocino earthquake, (b) the Kobe earthquake

flexible superstructure, whereas the right structure to have stiff superstructure. The examples of the results of the study are shown in Figs. 14 and 15. It can be seen from the figures that both isolated buildings are considerably influenced by structural pounding. The comparison between Figs. 4 and 14 as well as between Figs. 5 and 15 indicates that the influence of the base isolation on the structural response is significant. In particular, the values of the peak accelerations and pounding forces are substantially higher comparing to the case of non-isolated buildings. For both building, under all considered ground motions, the peak displacements and accelerations for the storeys increase up to a certain value of the gap distance and with further increase in the gap distance a decrease trend can be observed. The impact forces first increase with the increase in the gap

distance and then they show a decrease trend after passing a certain gap size value. All the storeys provide quite similar peak displacements and accelerations for all the considered gap distances. On the other hand, the peak pounding forces show significant differences between higher and lower storey levels. Regarding the left and the right isolated bases, it can be seen from Figs. 14 and 15 that the base peak displacements increase with the increase in the gap distances, whereas the curves of the base peak accelerations and peak pounding forces at the bases show the initial increase with further decrease trend as the gap size increases.

4. Conclusions

The study focused on the seismic response evaluation for isolated and non-isolated buildings considering the effect of pounding has been presented in this paper. In the analysis, inelastic three-storey structures with isolated and/or non-isolated bases and identical or different dynamic parameters of the superstructures have been considered.

The results of the study demonstrate that the variation of the peak storeys accelerations and displacements substantially depends on the type of the base. In the case of base-isolated building colliding with either isolated or non-isolated building, the variation of the storeys responses is relatively low. On the other hand, significant differences can be expected for the non-isolated building colliding with either isolated or non-isolated building.

The peak displacements and accelerations of the storeys of the isolated building with stiff superstructure remain nearly unchanged apart from the type of the base and structural properties of adjacent building. On the other hand, it has been noticed that there are differences between the responses of the isolated building with flexible superstructure due to pounding with the flexible non-isolated building and building with stiff superstructure with either isolated or non-isolated base. This clearly shows that the peak responses of the isolated building with flexible superstructure depends mainly on the structural parameters of adjacent building. The pounding-involved response of the isolated building with flexible superstructure contain contributions from both isolated base as well as from the superstructure (higher vibration modes). It has been observed that the flexibility of the superstructure tends to increase the peak storeys accelerations; however, this contribution is relatively low in comparison with the isolated base mode. Thus, the peak storeys accelerations of the base-isolated building with flexible superstructure become higher than the values obtained for the base-isolated building with stiff superstructure.

References

- Anagnostopoulos, S.A. and Karamaneas, C.E. (2008), "Use of collision shear walls to minimize seismic separation and to protect adjacent buildings from collapse due to earthquake-induced pounding", *Earthq. Eng. Struct. Dyn.*, **37**, 1371-1388.
- Bhaskararao, A.V. and Jangid, R.S. (2006), "Seismic analysis of structures connected with friction dampers", *Eng. Struct.*, **28**, 690-703.
- Buckle, I.G. and Mayes, R.L. (1990), "Seismic isolation: history, application and performance - a world overview", *Earthq. Spectra*, **6**, 161-202.
- Dimova, S.L. (2000), "Numerical problems in modelling of collision in sliding systems subjected to seismic excitations", *Adv. Eng. Softw.*, **31**, 467-471.

- Faravelli, L. (2001), "Modelling the response of an elastomeric base isolator", *J. Struct. Control.*, **8**, 17-30.
- Gueraud, R., Noel-Ieroux, J-P., Livolant, M. and Michalopoulos, A.P. (1985), "Seismic isolation using sliding elastomer bearing pads", *Nucl. Eng. Des.*, **84**, 363-377.
- Jangid, R.S. and Datta, T.K. (1995), "Seismic behavior of base-isolated buildings: a state-of-the-art review", *J. Struct. Build.*, **110**, 186-203.
- Jangid, R.S. and Londhe, Y.B. (1998), "Effectiveness of elliptical rolling rods for base-isolation", *J. Struct. Eng.*, **124**, 496-472.
- Jankowski, R. (2003), "Nonlinear rate dependent model of high damping rubber bearing", *Bull. Earthq. Eng.*, **1**, 397-403.
- Jankowski, R. (2005), "Non-linear viscoelastic modelling of earthquake-induced structural pounding", *Earthq. Eng. Struct. Dyn.*, **34**, 595-611.
- Jankowski, R. (2006), "Analytical expression between the impact damping ratio and the coefficient of restitution in the nonlinear viscoelastic model of structural pounding", *Earthq. Eng. Struct. Dyn.*, **35**, 517-524.
- Jankowski, R. (2008), "Earthquake-induced pounding between equal height buildings with substantially different dynamic properties", *Eng. Struct.*, **30**, 2818-2829.
- Jankowski, R., Wilde, K. and Fujino, Y. (2000), "Reduction of pounding effects in elevated bridges during earthquakes", *Earthq. Eng. Struct. Dyn.*, **29**, 195-212.
- Kelly, J.M. (1986), "Seismic base isolation: review and bibliography", *Soil Dyn. Earthq. Eng.*, **5**, 202-216.
- Komodromos, P. (2000), *Seismic isolation of earthquake-resistant structures*, WIT Press, Southampton.
- Komodromos, P. (2008), "Simulation of the earthquake-induced pounding of seismically isolated buildings", *Comput. Struct.*, **86**, 618-626.
- Komodromos, P., Polycarpou, P.C., Papaloizou, L. and Phocas, M.C. (2007), "Response of seismically isolated buildings considering poundings", *Earthq. Eng. Struct. Dyn.*, **36**, 1605-1622.
- Mahmoud, S., Chen, X. and Jankowski, R. (2008), "Structural pounding models with Hertz spring and nonlinear damper", *J. Appl. Sci.*, **8**, 1850-1858.
- Malhotra, P.K. (1997), "Dynamics of seismic impacts in base-isolated buildings", *Earthq. Eng. Struct. Dyn.*, **26**, 797-813.
- Matsagar, V.A. and Jangid, R.S. (2003), "Seismic response of base-isolated structures during impact with adjacent structures", *Eng. Struct.*, **25**, 1311-1323.
- Mostaghel, N. and Khodaverdian, M. (1987), "Dynamics of resilient-friction base isolator (R-FBI)", *Earthq. Eng. Struct. Dyn.*, **15**, 379-390.
- Mostaghel, N. and Tanbakuchi, J. (1983), "Response of sliding structure to earthquake support motion", *Earthq. Eng. Struct. Dyn.*, **11**, 729-748.
- Muthukumar, S. and DesRoches, R. (2006), "A Hertz contact model with nonlinear damping for pounding simulation", *Earthq. Eng. Struct. Dyn.*, **35**, 811-828.
- Nagarajaiah, S. and Sun, X. (2001), "Base-isolated FCC building: impact response in Northridge earthquake", *J. Struct. Eng.*, **127**, 1063-1075.
- Simo, J.C. and Kelly, J.M. (1984), "The analysis of multi-layer elastomeric bearings", *J. Appl. Mech.*, **51**, 256-262.
- Skinner, R.I., Tyler, R.G., Hiene, A.J. and Robinson, W.H. (1980), "Hysteretic dampers for the protection of structures from earthquakes", *Bull. New Zealand Soc. Earthq. Eng.*, **13**, 22-36.
- Tsai, H.C. (1997), "Dynamics analysis of base-isolated shear beams bumping against stops", *Earthq. Eng. Struct. Dyn.*, **26**, 515-528.
- Xu, Y.L., He, Q. and Ko, J.M. (1999), "Dynamic response of damper-connected adjacent structures under earthquake excitation", *Eng. Struct.*, **21**, 135-148.
- Zayas, A.V., Low, S.S. and Mahin, S.A. (1990), "A simple pendulum technique for achieving seismic isolation", *Earthq. Spectra*, **6**, 317-333.
- Zhang, W.S. and Xu, Y.L. (1999), "Dynamic characteristics and seismic response of adjacent structures linked by discrete dampers", *Earthq. Eng. Struct. Dyn.*, **28**, 1163-1185.